Spectral and spatial dynamics in InGaN blue-violet lasers

G. Ropars[a] and A. Le Floch
Laboratoire d'Electronique Quantique-Physique des Lasers, Unité Mixte de Recherche du Centre National de la Recherche Scientifique 6627, Université de Rennes 1, Campus de Beaulieu, F-35042 Rennes Cedex, France

G. P. Agrawal
The Institute of Optics, University of Rochester, Rochester, New York 14627

(Received 29 July 2006; accepted 1 November 2006; published online 15 December 2006)

An angular differential analysis of the longitudinal modes associated with successive spectral substructures in InGaN lasers demonstrates a large increase in the mode widths towards the red side of the spectra because of the antiguiding lens effects occurring in such gain-guided lasers. A simple model predicts the growing asymmetrical triangular-shape spectral envelope with much higher powers in the red substructures with increasing excitation, in agreement with the high-resolution spectral measurements. Moreover, the observed 20% mode-width variations imply a critical stripe-width limitation of the active medium that would prevent oscillation of higher-order modes on the blue side of the laser spectrum. © *2006 American Institute of Physics*.
[DOI: 10.1063/1.2404974]

Over the last decade, nitride-based blue semiconductor lasers first introduced by Nakamura[1] have attracted a good deal of attention because of their applications in electronics, optoelectronics, and optical-storage devices. Until now, most of these lasers have been fabricated by metal-organic chemical vapor deposition to lower the concentration of dislocations. It is expected that the optical properties of such gain-guided nitride lasers would be different from those of conventional double-heterostructure red lasers.[2] Although specific mode spectral properties of blue lasers have already been observed experimentally[3,4] and discussed theoretically,[5,6] several aspects are not yet well understood. In some cases, such lasers exhibit kinks and mode hopping with increasing excitation.[1] Moreover, the mode spectra seem to evolve and exhibit spectral substructures with mode bundles. In practice, high beam stability is claimed today for commercial blue lasers in which fundamental-mode operation is maintained using ion-implantation techniques to better control the laser geometry. However, the spectral evolution of these lasers remains unconventional and poorly understood. In this letter, we investigate the mode dynamics of such lasers using a wavelength-dependent differential analysis of the successive mode widths within the framework of a multisubstructure system. In particular, we try to isolate the physical mechanisms that govern the optical properties and to deduce from them an optimization procedure for the laser geometry.

Let us first present our spectral measurements on InGaN lasers from Sanyo. These gain-guided lasers exhibit a relatively low operating current and a stable beam structure. They operate in a fundamental transverse mode with a relatively low intensity noise. Their typical continuous-wave (cw) output power is about 5 mW at an excitation level of 1.2 times the threshold current I_{th} (37 mA for our specific laser). Figure 1(a) shows the high-resolution spectra of this diode at several excitation levels above threshold. The wavelength shift of about 0.02 nm/mA is rather weak compared to the usual shifts for other semiconductor lasers: for instance, the shifts are one order of magnitude larger for GaAlAs lasers. For this reason, in blue lasers it is easy to follow the relative evolution of the spectral substructures. Here we denote four substructures as depicted by the dotted lines in Fig. 1(a).

The physics of spectral substructures, i.e., an inhomogeneous broadening of the spectrum in nitride lasers, has recently been explained in terms of band-to-band transitions with a substantial broadening due to structural variation[7] and in terms of mode interference with the substrate.[8] We observe substructures with peak separation in the meV range, in agreement with the earlier observations.[1,8] Moreover, a relatively low intensity noise associated with this structure al-

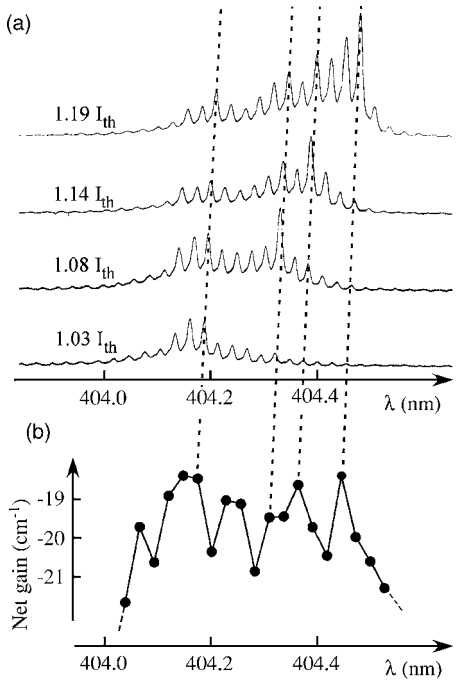

FIG. 1. Spectral substructure emission of an InGaN blue-violet laser. (a) High-resolution spectra as a function of the excitation current above the threshold I_{th}=37 mA, showing four mode bundles. (b) Net gain spectra for a subthreshold excitation measured by the Hakki-Paoli method.

[a]Electronic mail: guy.ropars@univ-rennes1.fr

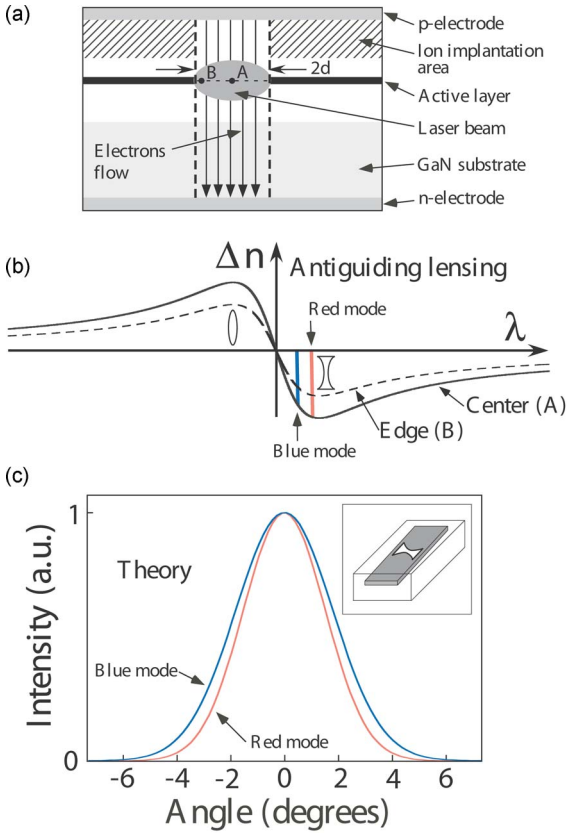

FIG. 2. (Color online) (a) Ion-implanted structure of the blue laser. (b) Schematic representation of the change of the refractive index at the center (point *A*) and at the edge (point *B*) of the laser beam vs the wavelength. (c) Expected normalized mode profiles in the junction plane on the red and blue sides of the oscillation region for a 20% mode-width variation using the near-planar representation of the laser cavity (Ref. 13). The inset schematizes the defocusing lens effect along the laser axis.

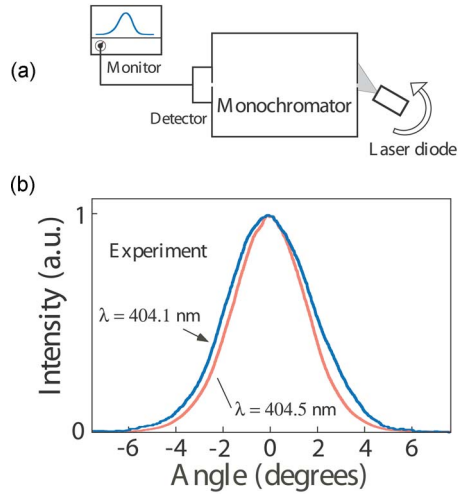

FIG. 3. (Color online) (a) Scheme of the experimental setup for the differential angular analysis. (b) Experimental normalized angular far-field patterns in the junction plane for red and blue side modes.

lows us to investigate these substructures on the gain curve in the subthreshold region, where it is possible to measure the active-medium net gain with the Hakki-Paoli method.[9,10] These measurements are shown in Fig. 1(b). We note the existence of the four mode bundles which successively generate the asymmetrical triangular-shape spectral envelops of Fig. 1(a). We conclude from this observation that the growth of the longest-wavelength substructure becomes more and more important with increasing current, keeping the linear polarization in the plane of the junction unchanged. We try to understand this typical behavior in the following discussion.

The structure of the ion-implanted InGaN laser is schematized in Fig. 2(a). The main geometrical parameter is the stripe width $2d$, whose values are 4.8 and 5.6 μm for the two lasers used here. By construction, the optical gain is maximum at the center of the stripe (point *A*). On the contrary, the gain vanishes at the edge of the electrically pumped region (point *B*). In such a gain-guided laser, as the oscillation occurs on the red side of the fluorescence profile, the wavelength dependence of the refractive indices at the center and at the edge of the active medium is schematized in Fig. 2(b). Note that a red mode will experience a divergent defocusing greater than the one for a blue mode during their propagation along the active medium, leading to a larger mode width in the laser diode for the red mode. In the frame of the parabolic approximation for the transverse index variation, the fundamental mode will be affected by different relative defocusing effects according to the wavelength. Although the transverse dimension suggests a waveguide approach, we expect mode-width variations similar to those found for nearly planar resonators.[11] Even relatively weak divergent focal-length variations, resulting from small refractive index changes in a semiconductor, lead to large mode-width variations for the fundamental mode.[12] This behavior is shown in Fig. 2(c) on the mode profiles outside the laser.

To test for spatial width variations, we performed a high-resolution differential angular analysis of different oscillating modes, from the blue side to the red side of the spectrum, using the experimental setup shown in Fig. 3(a). The laser is mounted on a rotation stage controlled by a computer. Figure 3(b) shows the observed large beam divergence variations of the order of 20% for two wavelengths separated by only 0.4 nm. The experimental beam widths, deduced from the usual Gaussian beam approximation for the whole spectrum, are shown in Fig. 4(b). Note that the variations of this fundamental parameter follow the relative mode intensity variations displayed in Fig. 4(a) for an excitation of $1.19I_{\mathrm{th}}$. The contribution of the four spectral substructures is clear in this case.

Within the framework of a simple model, one can then express the output power P_i for different modes as

$$P_i = Kw_i(g_i - g_{\mathrm{th}}), \tag{1}$$

where g_{th} is the gain at the threshold, g_i and w_i are the gain and the width of the ith mode, respectively, and K a constant. Unfortunately, to compare the expected power values with the experimental mode powers, we cannot employ the Hakki-Paoli measurements of the net gain at an excitation of $1.19I_{\mathrm{th}}$ because that method can be used only below threshold. However, it is well known that the threading dislocations shorten the lifetime of blue lasers through an increase of the threshold current density.[13] For one of our lasers, we observe this type of degradation. Nevertheless, this laser can still allow us to record the evolutions of the different mode bundles at an excitation current corresponding to $1.19I_{\mathrm{th}}$ for a nondegraded laser. We can deduce the effective net gain variations for the oscillating laser diode above threshold by taking into account the reduced losses, as shown in Fig. 4(c). We note that the relative gain of the red substructures really increases in our lasers. When introduced in Eq. (1), the estimated spectral profile for the blue laser at $1.19I_{\mathrm{th}}$ is shown by the open

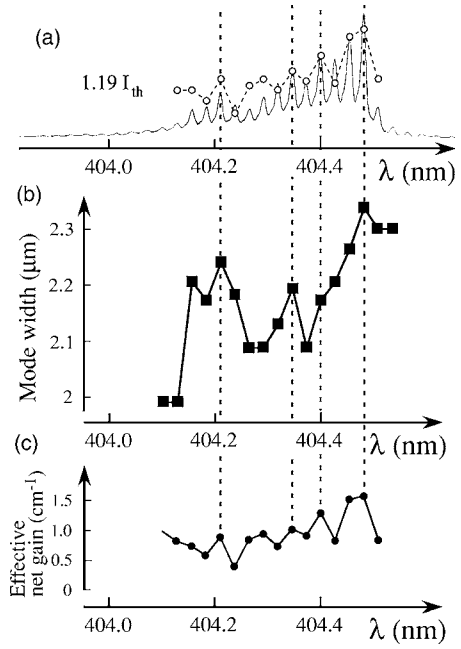

FIG. 4. (a) Typical asymmetrical triangular mode spectrum at $1.19I_{th}$. The open circles show the estimated theoretical spectral profile using Eq. (1). (b) Corresponding individual mode-width variations in the junction plane. (c) Effective net-gain curve recorded at the same injection current using a degraded laser.

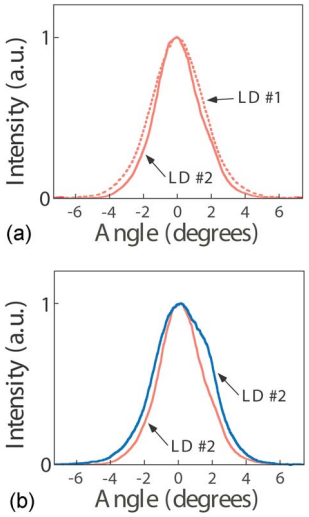

FIG. 5. (Color online) (a) Comparative normalized intensity angular distribution for 4.8 μm (laser 1) and 5.6 μm (laser 2) stripe widths both on the red side of the spectrum at $1.19I_{th}$. (b) Comparative results for the same laser 2 for the red and blue sides of the oscillating region. The 5.6 μm stripe width of this diode is too large to ensure fundamental operation for the blue mode (see the deformation).

circles in Fig. 4(a). Clearly, by taking into account both the inhomogeneous broadening of the gain and the individual mode widths, one can explain the typical asymmetrical triangular spectral envelope characterizing these nitride lasers. The higher mode intensities on the red side correspond to the larger mode widths oscillating on the lower energy spectral substructures because of the defocusing effects induced by refractive index variations. To increase the output power, one may wonder if it is possible to further increase the stripe width, or if there is a limitation on the width of such an active medium.

Let us recall that most applications require laser operation in the fundamental spatial mode to avoid higher-order lateral modes.[14,15] The large mode-width variations observed here may play a role in this context. To illustrate this, we compare the behavior of two slightly different blue lasers from Sanyo. The ion-implantation technique imposes an active stripe width of 4.8 μm for diode 1, and 5.6 μm for diode 2. The angular mode profiles of both lasers, on the red side, are shown in Fig. 5(a). The observed 16% difference in the beam widths at $1/e^2$ point is in agreement with the respective geometries. However, the corresponding profile on the blue side shows a limitation on the possible increase in stripe width. Indeed, for the larger stripe of diode 2, the first-order lateral mode starts to be generated specifically on the blue side, where the mode widths are the smallest [Fig. 5(b)]. Thus, our angular investigation of the individual mode profiles is a useful method for testing the optimization of the stripe widths of the active medium.

In conclusion, the mode spectral substructure evolution in gain-guided blue lasers is governed by both the inhomogeneous broadening of the gain and by the mode-width variations. The differential angular analysis is a powerful tool for understanding the behavior of these lasers and for optimizing the active-medium dimensions. Such mode dynamics are expected to occur in similar gain-guided nitride lasers including recent UV lasers[16,17] and envisioned far-UV lasers.[18]

The authors would like to thank J. P. Taché and F. Rogister for their constructive discussions and A. Carré and M. Lepareur for their help. This work was supported jointly by the U.S. National Science Foundation under Grant No. INT-0003636, by CNRS Grant No. 10675, and by the Programme Pluriformations 841P.

[1] See S. Nakamura and G. Fasol, *The Blue Laser Diode* (Springer, Heidelberg, 1997).
[2] G. P. Agrawal and N. K. Dutta, *Semiconductor Lasers* (Kluwer Academic, New York, 1993), Chap. 1.
[3] S. Nakamura, Appl. Phys. Lett. **70**, 2753 (1997).
[4] C. Eichler, S.-S. Schad, F. Scholz, D. Hofstetter, S. Miller, A. Weimar, A. Lell, and V. Härle, IEEE Photonics Technol. Lett. **17**, 1782 (2005).
[5] H. X. Jiang and J. Y. Lin, Appl. Phys. Lett. **74**, 1066 (1999).
[6] K.-G. Gan, C.-K. Sun, S. P. DenBaars, and J. E. Bowers, Appl. Phys. Lett. **84**, 4675 (2004).
[7] B. Witzigmann, V. Laino, M. Luisier, U. T. Schwarz, G. Feicht, W. Wegscheider, K. Engl, M. Furitsch, A. Leber, A. Lell, and V. Härle, Appl. Phys. Lett. **88**, 021104 (2006).
[8] U. T. Schwarz, E. Sturm, W. Wegscheider, V. Kümmler, A. Lell, and V. Härle, Appl. Phys. Lett. **83**, 4095 (2003).
[9] B. W. Hakki and T. L. Paoli, J. Appl. Phys. **44**, 4113 (1973).
[10] S. Nakamura, MRS Internet J. Nitride Semicond. Res. **2**, 5 (1997).
[11] A. Le Floch, A. Daudé, R. Le Naour, J. M. Lenormand, and G. Ropars, J. Opt. Soc. Am. B **2**, 503 (1985).
[12] J. P. Taché, A. Le Floch, and R. Le Naour, Appl. Opt. **25**, 2934 (1986).
[13] J. S. Speck and S. J. Rosner, Physica B **273–274**, 24 (1999).
[14] W. W. Chow and H. Amano, IEEE J. Quantum Electron. **37**, 265 (2001).
[15] J. Piprek, R. K. Sink, M. A. Hansen, J. E. Bowers, and S. P. DenBaars, Proc. SPIE **3944**, 28 (2000).
[16] H. Amano, A. Miyazaki, K. Iida, T. Kawashima, M. Iwaya, S. Kamiyama, I. Akasaki, R. Liu, A. Bell, F. A. Ponce, S. Sahonta, and D. Cherns, Phys. Status Solidi A **201**, 2679 (2004).
[17] M. Iwaya, K. Iida, T. Kawashima, A. Miyazaki, H. Kasugai, S. Mishima, A. Honshio, Y. Miyake, S. Kamiyama, H. Amano, and I. Akasaki, Phys. Status Solidi C **7**, 2828 (2005).
[18] Y. Taniyasu, M. Kasu, and T. Makimoto, Nature (London) **441**, 325 (2006).